ICIC Express Letters ICIC International ©2020 ISSN 1881-803X
Volume **14**, Number **7**, July **2020** pp. **661–668**

DISTRIBUTED COOPERATIVE FORMATION CONTROL FOR MULTI-AGENT SYSTEMS BASED ON ROBUST ADAPTIVE STRATEGY

Weizhen He[1], Bing Yan[2] and Chengfu Wu[1]

[1]School of Automation
Northwestern Polytechnical University
No. 127, West Youyi Road, Beilin District, Xi'an 710072, P. R. China
wu.nwpu@gmail.com

[2]School of Electronic and Electrical Engineering
The University of Adelaide
Adelaide, South Australia 5005, Australia

Received January 2020; accepted April 2020

Abstract. *In this study, a distributed robust cooperative control based on robust adaptive strategy is investigated for multi-agent systems (MASs) to achieve formation consensus and formation transformation according to the reference formation. Firstly, a graph theory-based distributed adaptive protocol together with a no-grid collision-free method is proposed to form formations and avoid collisions with obstacles. Then, an adaptive strategy based on L_1 robust control is developed for improving robustness against system uncertainties and interferences. Finally, the new control schemes are applied to multi-robot systems consisting of unmanned two-wheeled balancing robots. The resulting closed-loop multi-agent system is stable. The effectiveness of the new cooperative control behavior strategy and its robustness are verified by simulations.*
Keywords: MASs, Distributed cooperative control, Formation control, Robust adaptive strategy

1. **Introduction.** In general, a multi-agent system (MAS) refers to a computerized system composed of multiple interacting intelligent agents, and compared with traditional single complex individuals, multiple agents work together to improve operational efficiency and reduce consumption. The group behavior to accomplish a certain common goal is called the cooperative control of MAS.

With the wide application of collaborative control for MASs in various fields, the collaborative formation control of MASs has become a research hotspot in the control field. At present, most of the mature optimization algorithms are based on leader-follower [1-4]. However, the robustness of this method is limited. Once the leader is abnormal, the formation will not be realized, and the whole MAS has the risk of failure. Another mainstream method is centralized method [5-7]. The centralized method, however, requires to collect the data on the agent in the network and process it in a fusion center, which brings many restrictions.

Compared with centralized methods, distributed methods are relatively inexpensive to implement with more robustness and flexibilities [8,9]. In [10], an adaptive distributed formation control method was discussed. The result in [11] investigated a protocol and a control law for a single robot so that a team of such robots can interact and cooperate to reach the displacement from an eligible reference formation. Furthermore, the free collision is another requirement for formation control [12]. A coordinated formation flight and obstacle avoidance control were investigated for the multi-UAV system in [13]. The

DOI: 10.24507/icicel.14.07.661

works of the non-grid method were proposed in [14,15], where no division of the map is used to minimize the energy of obstacle avoidance for MASs.

Generally, it is difficult to get accurate modeling of the actual system. The uncertainties and external disturbance have a great influence on dynamics of systems, especially for MASs due to the increasing number of agents and system equipment. The traditional PID controller has limited ability of anti-interference [16,17]. Therefore, the robustness of controller is an important requirement for design and implementation of system stability and coordinated control. The work in [18] proposed a sliding mode control with strong robustness. However, there are oscillations in the output of the controller. Using L_1 adaptive controller could well suppress the inaccuracy of model parameter design and external interferences [19,20]. Most of the L_1 adaptive control methods are applicable to single-input single-output (SISO) systems. Theoretical challenges arise from complex multi-input multi-output (MIMO) systems and high robustness requirements against uncertainties and external disturbance.

Motivated by the observation, we propose a distributed robust coordination formation control to achieve formation consensus and obstacle avoidance under the system uncertainties and external interference. The major contributions of this research can be generalized as follows:

1) Developing a graph-based distributed formation control method to form and keep different formations for MASs;

2) Presenting an on-line non-grid method together with optimal formation changing strategies to avoid collision with both obstacles and other agents;

3) Providing L_1 robust adaptive control for MIMO multiple two-wheeled balancing robots against system uncertainties and external interference, during formation keeping and changing.

The organization of this paper is as follows. In Section 2, the mathematical model of two-wheeled vehicles is established, and the formation consensus problem is presented. In Section 3, an adaptive mapping formation protocol and the distributed consensus control law are designed. We also propose an optimal collision-free algorithm and the L_1 adaptive control architecture for the motion control of robots. The proposed robust consensus formation control strategies with obstacle avoidance are compared with PID control using simulation in Section 4. Section 5 offers the conclusion of this paper.

2. **Problem Statement and Preliminaries.**

2.1. **System description.** According to [21], the mathematical model of two-wheeled vehicles is established as

$$\begin{aligned}
&\left(2M + \frac{2J_\phi}{R^2} + m\right)\ddot{x}_m + mL\ddot{\theta} = \frac{C_L + C_R}{R} \\
&J_P\ddot{\theta} + mL^2\ddot{\theta} - mgL\theta = -mL\,\ddot{x}_m \\
&\left(DM + \frac{DJ_\phi}{R^2} + \frac{2J_\psi}{D}\right)\ddot{\psi} = \frac{C_L - C_R}{R}
\end{aligned} \tag{1}$$

where C_L, C_R indicate the torques of left and right wheel, D is the distance between two wheels, L is the distance between the axis center and mass center, m denotes quality of the vehicle besides wheels, R is the radius of left and right wheels, and J_ϕ, J_P, J_ψ represent moment of inertia of wheels, pendulum and body, respectively. M is the quality of the left and right wheels, θ denotes inclination angle between swing bar and z plane, ψ denotes the azimuth, and x_m indicates the average displacement of wheels.

The ground mobile robot model can be simplified as

$$\dot{X}_i = A_iX_i + B_iU_i, \quad Y_i = C_i^TX_i, \quad i = 1, 2, \dots, n \tag{2}$$

where $X_i = \left[p_i, \theta_i, \dot{p}_i, \dot{\theta}_i, \psi_i, \dot{\psi}_i\right]^T$, $U_i = [C_L, C_R]$, p_i indicates the position. We set $M = 0.8$ kg, $R = 0.1$ m, $L = 0.5$ m, $J_\psi = 0.001$ kg·m^2, $m = 10$ kg, $J_\phi = 0.002$ kg·m^2, $J_P = 0.0034$ kg·m^2, $D = 0.5$ m.

2.2. **Problem description.** The first problem we concern is formation consensus with obstacle avoidance defined in Definition 2.1. The robustness of the controller is the other problem of this paper to against the uncertainties of system and external interferences.

Definition 2.1. *For MAS with n robots from p_1 to p_n, the system has progressively achieved the formation consensus among reference formations $F(t)$ under optimal energy consumption function M, if condition (3) is met*

$$\begin{aligned} &\lim_{t\to\infty} [x_i, y_i]^T - [x_j, y_j]^T = d' - d'', \quad d', d'' \in F(t) \quad i, j = 1, 2, \ldots, n \\ &\lim_{t\to\infty} [x_i, y_i]^T - [x_c, y_c]^T = 0 \quad \text{s.t. } Min\left(\|[x_i, y_i]^T - [x_o, y_o]^T\|\right) > R_{safe}, \ i = 1, 2, \ldots, n \end{aligned} \tag{3}$$

where (x_i, y_i) denotes the position of agent p_1, and $F(t)$ presents the predesigned formations. The objective position and the excluding object are (x_c, y_c) and (x_o, y_o), respectively.

3. **Main Results.** In this paper, the system overview of the proposed method is shown in Figure 1. The design of the main function block is given one by one in this section.

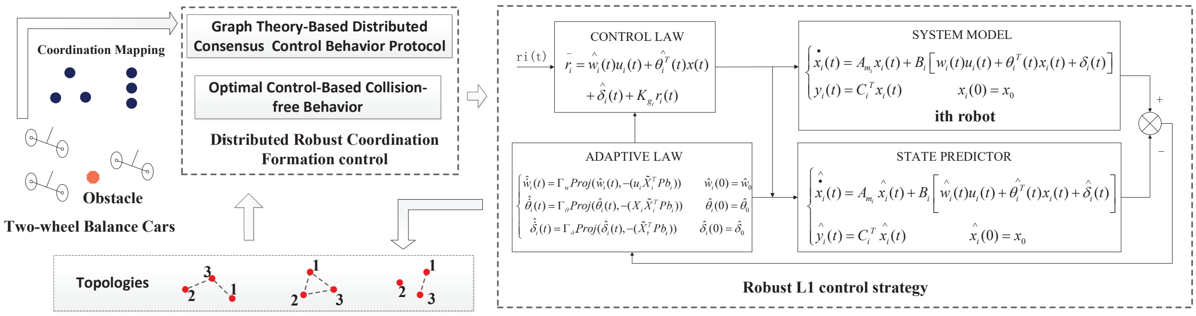

Figure 1. System overview

3.1. **Graph theory-based distributed consensus control behavior protocol.** The interaction topology of the MASs is naturally modelled as a dynamic directed graph $G(t)$ with nodes $V(t)$, edges $E(t)$ and adjacency matrix $A(t) = a_{ij}(t)$. Each node can be regarded as a two-wheeled balancing robot. Therefore, the formation control of the robot can be divided into two steps: the first step is the formation consensus control of the nodes, and the second step is the position control of the robot. This section focuses on formation conformance control protocol. Set $P_i \in R^{2\times 1}$, $i = 1, \ldots, n$ is the positions of n robots.

We assume that there exists an infinite sequence of uniformly bounded, nonoverlapping time intervals and the union of the dynamic topologies $G(t)$ has a spanning tree over each interval. This assumption is given for MASs to achieve consensus under dynamic topologies [22].

For $P_j \in g(P_i)$, if $a_{ij}(t) = 1$, then we call $g(P_i)$ a group of P_i. For formation control, formation mapping $d(P) = M(P)F$ is very important to determine the relative position of different agents in formation. Formation matrix $F(t) = f_i$, $i = 1, 2, \ldots, k$ is k types formations, each of which consists of basic points. For instance, f_1 is set as a triangle with 3 points, while f_2 is set as a straight line with 3 points, each of which has a different basic area.

The adaptive mapping formation protocol is designed as Theorem 3.1.

Theorem 3.1. *The adaptive protocol is used to map P to $d(P)$ according to designed formation $F(t)$.*

$$\begin{array}{c} d(g(P_1)) = \arg\min\limits_{d(g(P_1))\in F} L^F(g(P_1)) \\ d(g(P_2)) = \arg\min\limits_{d(g(P_2))\in F} L^F_{d(g(P_1))}(g(P_2)) \\ \cdots \\ d(g(P_n)) = \arg\min\limits_{d(g(P_n))\in F} L^F_{d(g(P_1))\oplus\cdots\oplus d(g(P_n))}(g(P_n)) \end{array}, \\ d(P) = d(g(P_1)) \cup \cdots \cup d(g(P_n)) \\ L^F(g(P_i)) = \sum a_{ij}(t)\,\|\delta P\| \\ L^F_{d(g(P_k))}(g(P_i)) = \overset{d(g(P_k))\rightharpoonup d(g(P_i))}{\sum a_{ij}(t)} \quad \|\delta P\| \\ \delta P = (P_j - P_i) - (d(P_j) - d(P_i)) \tag{4}$$

where P_i is mapped to $d(P_i)\in F$. A is coordinated in B by $A \rightharpoonup B$, if $d^A(P_j) - d^A(P_i) = d^B(P_j) - d^B(P_i)$ for any $P_i, P_j \in A$, any $P_i, P_j \in B$, $d^A(P_i)\in d(A)$, $d^B(P_i)\in d(B)$. We have $C = A\oplus B = \{c_1, c_2, \ldots\}$, where $c\in A$ or $c\in B$ for any $c\in C$. If B is eligible, the eligibility of $A\oplus B$ will be guaranteed. See [11,15] for detailed description.

In order to achieve consensus based on relative position of formation, u_i^1 is designed for the ith robot.

$$u_i^1 = \sum_{j=1}^{n} a_{ij}(t)\frac{\left(\tilde{P}_j - \tilde{P}_i\right)}{\left\|\tilde{P}_j - \tilde{P}_i\right\|} \tag{5}$$

where $\tilde{P}_i = P_i - d(P_i)$, $\tilde{P}_j = P_j - d(P_j)$ are the errors of formation consistency for i, j robots.

Similarly, the behavior of following the target can be seen as a virtual navigator fully connected to the robot. The element of its adjacency matrix is 1, so we can get u_i^2 as

$$u_i^2 = \frac{(P_i^c - P_i)}{\|P_i^c - P_i\|} \tag{6}$$

where P_i^c is the objective reference for the ith robot.

3.2. **Optimal collision-free control.** In terms of collision-free control strategy, each agent is able to avoid obstacles and avoid collision with other agents. We define the following areas.

Obstacle range

$$\Delta = \left\{x | x\in R^3, \|x - c_k\| \le r + r_{ob}\right\}$$

Detection range

$$\Gamma_o = \left\{x | x\in R^3, r + r_{ob} \le \|x - c_k\| \le R + r_{ob}\right\}$$

Safety range

$$\Pi = \left\{x | x\in R^3, \|x - c_k\| \ge R + r_{ob}\right\}$$

where R represents the radius of the detection range, and the geometric center of the kth collision object is $c_k\in\Omega$. Ω presents the set of those centres of obstacles and agents excluding agent i.

$$r_{ob} = \begin{cases} r, & \text{if it may collide with an agent} \\ r_{oj}, & \text{if it may collide with the } j\text{th obstacle} \end{cases}$$

where r_{oj} denotes the radius of the jth obstacle of q obstacles.

The penalty on obstacles is designed as

$$f(E)=\sum_{i=1}^{n}\sum_{k=1}^{n+q-1}m_i^k(E)\geq 0,\quad m_i^k(E)=\begin{cases}0, & P_i\in\Pi\\ e^{\left(\frac{(R+r_{ob})^2-\|P_i-c_k\|}{\|P_i-c_k\|^2-(r+r_{ob})^2}\right)}-1, & P_i\in\Gamma_o\end{cases}\tag{7}$$

Based on our work in [15], the optimal collision-free control input u_i^3 is given in (8). As the reasonable contraction transformation formation is beneficial to the obstacle avoidance of the whole MAS, the reference formation will switch to the minimum basic area formation when encountering obstacles in order to better avoid obstacles, such as linear formation.

$$u_i^3=\begin{cases}0, & P_i\in\Pi\\ -e^{\left(\frac{(R+r_{ob})^2-\|P_i-c_k\|^2}{\|P_i-c_k\|^2-(r+r_{ob})^2}\right)^2}\frac{4\left((R+r_{ob})^2-(r+r_{ob})^2\right)\left((R+r_{ob})^2-\|P_i-c_k\|^2\right)}{\left(\|P_i-c_k\|^2-(r+r_{ob})^2\right)^3}(P_i-c_k), & P_i\in\Gamma_o\end{cases}\tag{8}$$

Therefore, the control input for the ith agent regarded as a point is designed as

$$u_i=u_i^1+u_i^2+u_i^3\tag{9}$$

Remark 3.1. *Notice that the control input u_i can be regarded as a combination of three behaviors, u_i^1 is a consensus control input based on the relative position of formation, u_i^2 is a tracking target control input, and u_i^3 is an optimal obstacle avoidance control behavior under the combination of three behaviors. If there is no obstacle, the local-based error vector divided by its modulus is an adaptive method to adjust control parameters. The proof of the consensus is shown in [11]. Meanwhile, when obstacles are considered, the proof of the formation stability and the optimization of obstacle avoidance algorithm are shown in our research [15].*

3.3. **Robust L_1 control schemes for two-wheeled balancing robot.** In this section, the L_1 adaptive control architecture is developed for the motion control of robots to improve the robustness against uncertainties and disturbances. The adaptive architecture adapts fast leading to desired transient performance for the system control signals and states simultaneously. The structure is suitable for both SISO systems and MIMO systems. The dynamics for the ith channel can be written as

$$\begin{cases}\dot{X}_i(t)=A_{m_i}X_i(t)+B_i\left[w_i(t)u_i(t)+\theta_i(t)X_i(t)+\delta_i(t)\right]\\ Y_i(t)=C_i^TX_i(t)\qquad X_i(0)=X_0\end{cases}\tag{10}$$

where $A_{m_i}=A_i-B_iK_i$; we have

$$\begin{cases}\dot{\hat{X}}_i(t)=A_{m_i}\hat{X}_i(t)+B_i\left[\hat{w}_i(t)u_i(t)+\hat{\theta}_i(t)X_i(t)+\hat{\delta}_i(t)\right]\\ \hat{Y}_i(t)=C_i^T\hat{X}_i(t)\qquad \hat{X}_i(0)=X_0\end{cases}\tag{11}$$

where $\hat{w}_i(t)$, $\hat{\theta}_i(t)$, $\hat{\delta}_i(t)$ are the adaptive parameters. The adaptive laws are

$$\begin{cases}\dot{\hat{w}}_i(t)=\Gamma_w Proj\left(\hat{w}_i(t),-\left(u_i\tilde{X}_i^TPb_i\right)\right) & \hat{w}_i(0)=\hat{w}_0\\ \dot{\hat{\theta}}_i(t)=\Gamma_\theta Proj\left(\hat{\theta}_i(t),-\left(X_i\tilde{X}_i^TPb_i\right)\right) & \hat{\theta}_i(0)=\hat{\theta}_0\\ \dot{\hat{\delta}}_i(t)=\Gamma_\delta Proj\left(\hat{\delta}_i(t),-\left(\tilde{X}_i^TPb_i\right)\right) & \hat{\delta}_i(0)=\hat{\delta}_0\end{cases}$$

in which $\tilde{X}_i(t)=\hat{X}_i(t)-X(t)$ represents the tracking error between the system dynamics in (11) and the state predictor, $\Gamma>0$ denotes the adaptations gain, and $P^T>0$ is the solution of the algebraic Lyapunov equation $A_{m_i}^TP_i+P_iA_{m_i}=-Q$, $Q>0$. This ensures the stability of motion control of robots.

4. **Numerical Example.** In this section, three two-wheeled balancing robots are used to verify the proposed robust cooperative formation control strategies with obstacle avoidance. The PID control is used to compare with our method based on L_1 adaptive control.

In the simulation, the initial states of the robots are $[2,0,0,0,20,0]^T$, $[1,0,0,0,10,0]^T$, $[-3,0,0,0,-20,0]^T$, and the objective movement of formation is $[0,0,1,0,45,0]^T$. The obstacles are located in $(24,30)$, $(30,33)$, $(34,36)$, $(33.5,27)$, $(36,28)$, $(31,22.5)$. The radius r of obstacles and agents are $[1,1.2,1,1,1,1.5]$ and $[0.5,0.5,0.5]$, respectively. The detection radius R of agents is $[3.5,3.5,3.5]$. The specified reference formations are switched between equilateral triangles with a vertex angle of 120 degrees and straight lines to avoid collision. The communication topology for the robots is undirected graph that is fully connected, which is fixed topology.

For two-wheeled balancing robot system, the pole of the A matrix is $(0,0,10.8004,-10.8004,0,0)$. Therefore, the system is not stable. We use LQR method to realize state feedback and assign poles to $(-101.56,-1.38+0.0094,-1.38+0.0094,-1.09,-0.3162,-39.6987)$.

$$K=\begin{bmatrix} -3.162 & -53.294 & -6.067 & -13.665 & 0 & 0 \\ 0 & 0 & 0 & 0 & 1 & 3.241 \end{bmatrix}$$

Setting system model uncertainty parameters: $w(t)=[1\ 1]$,

$$\theta(t)=\begin{bmatrix} 0.1*\sin(\mathrm{pi}*\mathrm{u}/2) & 0 & 0 & 0 & 0 & 0 \\ 0 & 0 & 0 & 0 & 0.5*\sin(\mathrm{pi}*\mathrm{u}/4) & 0 \end{bmatrix}^T,$$

$\delta(t)$ is Band-Limited White Noise. We can get $\theta_{\max}=0.6$, $\Gamma=5000$, $kg=[13.1626,1]^T$, when we set $k_1=90$, $k_2=100$, $\lambda=\left\|\bar{G}(s)\right\|_{L1}\|\theta\|_{L1}=0.6006<1$. By adopting PID motion control and robust L_1 adaptive method, the simulation of robust formation control and PID-based formation control are given, respectively.

The result of PID-based formation control is shown in Figure 2. Under PID based formation control, the three robots could basically keep the triangular formation moving along the specified route. For obstacle avoidance strategies, they change to a straight line while avoiding obstacles, and keep the triangle before and after avoiding obstacles. However, in the presence of system uncertainties and noise disturbances, the position state of the robots and formation errors oscillate greatly. To make matters worse, the collision could happen between the robots and obstacles due to the shocks caused by system uncertainties and interference.

As we can see from Figure 3, the three robots form the specified triangular formation from the initial state under L_1 adaptive formation control. When obstacles are detected,

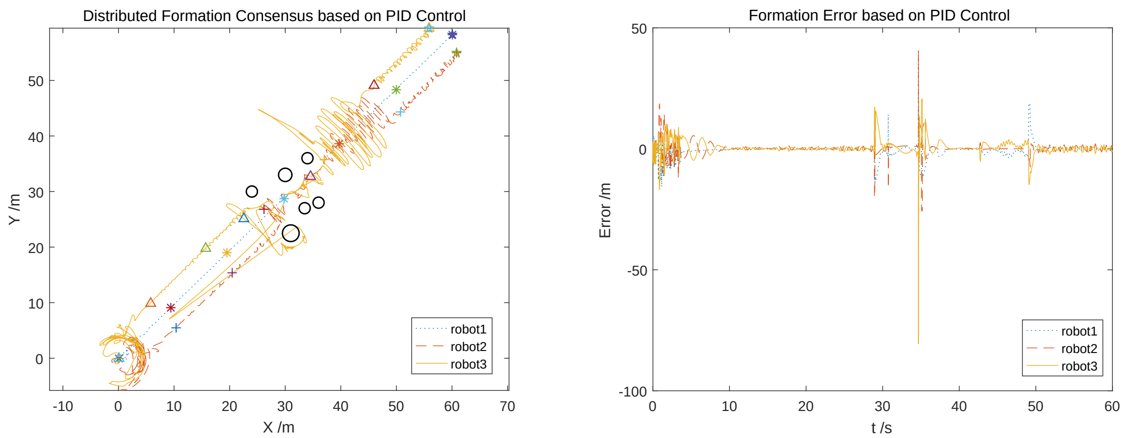

FIGURE 2. Distributed formation consensus and formation error based on PID control

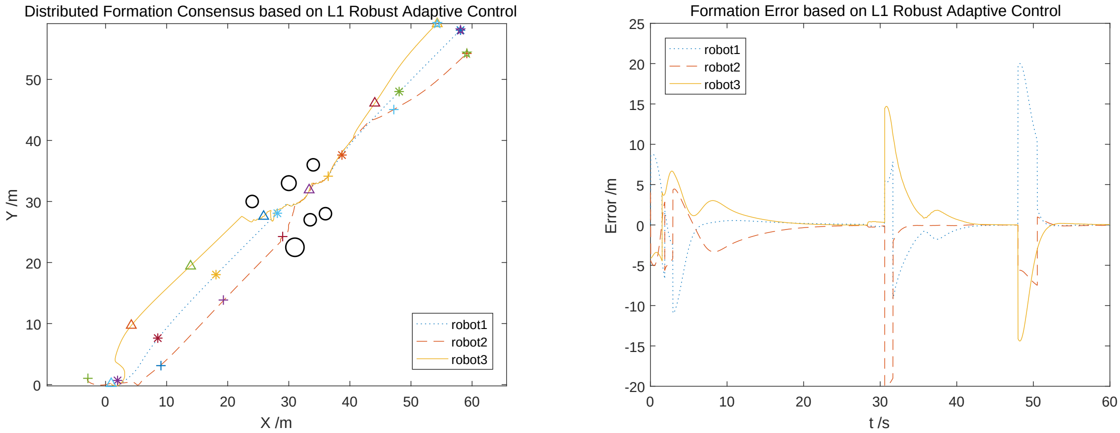

FIGURE 3. Distributed formation consensus and formation error based on L_1 robust adaptive control

the formation changes from the specified triangle to the smallest straight line. The three cars avoid the obstacles in a straight line formation, and in the absence of new obstacles within 3 seconds, they change back to the designated triangular formation and move forward in accordance with the designated trajectory. The error of formation has fluctuated in the stage of obstacle avoidance, and finally converges to zero.

5. **Conclusions.** In this paper, we have proposed a robust cooperative formation control method for MASs against interference and uncertainties. A distributed formation consensus protocol is designed for robots to keep formations while tracking reference targets. A no-grid obstacle avoidance algorithm and formation transformation strategy are proposed to solve the collision-free formation problem. Based on L_1 adaptive control, a robust controller is designed for two-wheeled balancing robot system such that the resulting closed-loop system is asymptotically stable with interferences and uncertainties. Compared with PID-based formation control, simulation results have shown that the new design scheme proposed can lead the MAS to achieve cooperative formation collisions-free formation consensus with robustness against interferences and uncertainties. This paper discusses the formation consensus problem in the case of fixed topology; the switching topology will be studied in the future.

REFERENCES

[1] K. Shojaei, Leader-follower formation control of under actuated autonomous marine surface vehicles with limited torque, *Ocean Engineering*, vol.105, pp.196-205, 2015.

[2] A. Mahmood and Y. Kim, Leader-following formation control of quadcopters with heading synchronization, *Robotics and Autonomous System*, vol.47, pp.68-74, 2015.

[3] G. Wen, C. L. P. Chen, J. Feng et al., Optimized multi-agent formation control based on an identifier-actor-critic reinforcement learning algorithm, *IEEE Trans. Fuzzy Systems*, vol.26, no.5, pp.2719-2731, 2018.

[4] Z. Han, K. Guo, L. Xie et al., Integrated relative localization and leader-follower formation control, *IEEE Trans. Automatic Control*, vol.64, no.1, pp.20-34, 2018.

[5] H. Wang, W. Sun, X. Lin et al., A centralized multi-sensor particle filter algorithm of formation targets, *International Conference on Digital Information and Communication Technology and Its Applications*, pp.50-55, 2016.

[6] A. S. Branda, Sarcinelli-Filho and Mario, On the guidance of multiple UAV using a centralized formation control scheme and Delaunay triangulation, *Journal of Intelligent and Robotic Systems: Theory and Applications*, vol.84, nos.1-4, pp.397-413, 2016.

[7] B. M. Ferreira, A. C. Matos, N. A. Cruz et al., A centralized approach to the coordination of marine robots, *Lecture Notes in Electrical Engineering*, pp.567-576, 2015.

[8] Y. Liu, J. M. Montenbruck, D. Zelazo et al., A distributed control approach to formation balancing and maneuvering of multiple multirotor UAVs, *IEEE Trans. Robotics*, vol.34, no.4, pp.870-882, 2018.

[9] X. Dong, B. Yu, Z. Shi et al., Time-varying formation control for unmanned aerial vehicles: Theories and applications, *IEEE Trans. Control Systems Technology*, vol.23, no.1, pp.340-348, 2015.

[10] Z. Peng, S. Yang, G. Wen et al., Adaptive distributed formation control for multiple nonholonomic wheeled mobile robots, *Neurocomputing*, vol.173, pp.1485-1494, 2016.

[11] H. Yu, P. Shi and C. C. Lim, Scalable formation control in stealth with limited sensing range, *International Journal of Robust and Nonlinear Control*, vol.27, no.3, pp.410-433, 2017.

[12] L. Liu, C. Luo and F. Shen, Multi-agent formation control with target tracking and navigation, *IEEE International Conference on Information and Automation*, pp.98-103, 2017.

[13] Y. Kuriki and T. Namerikawa, Consensus-based cooperative formation control with collision avoidance for a mutil-UAV system, *American Control Conference*, pp.4-6, 2014.

[14] Y. Chen and J. Sun, Distributed optimal control for multi-agent systems with obstacle avoidance, *Neurocomputing*, vol.173, pp.2014-2021, 2016.

[15] B. Yan, P. Shi, C. Lim et al., Optimally distributed formation control with obstacle avoidance for mixed-order multi-agent systems under switching topologies, *IET Control Theory and Applications*, vol.12, no.13, pp.1853-1863, 2018.

[16] R. H. Stone, The T-Wing tail-sitter research UAV, *Biennial International Powered Lift Conference and Exhibit*, pp.1-10, 2002.

[17] K. Kita, A. Konno and M. Uchiyama, Hovering control of a tail-sitter VTOL aerial robot, *Journal of Robotics and Mechatronics*, vol.21, no.2, pp.277-283, 2009.

[18] J. A. Guerrero, R. Lozano, G. Romero et al., Robust control design based on sliding mode control for hover flight of a mini tail-sitter unmanned aerial vehicle, *The 35th Annual Conference of IEEE*, pp.2342-2347, 2009.

[19] C. Cao and N. Hovakimyan, Design and analysis of a novel L1 adaptive control architecture with guaranteed transient performance, *IEEE Trans. Automatic Control*, vol.53, no.2, pp.586-590, 2008.

[20] C. Cao and N. Hovakimyan, Design and analysis of a novel L1 adaptive controller, Part I: Control signal and asymptotic stability, *American Control Conference*, pp.3397-3402, 2006.

[21] K. D. Do and G. Seet, Motion control of a two-wheeled mobile vehicle with an inverted pendulum, *Journal of Intelligent and Robotic Systems*, vol.60, nos.3-4, pp.577-605, 2010.

[22] W. Ren and R. W. Beard, Consensus seeking in multi-agent systems under dynamically changing interaction topologies, *IEEE Trans. Automatic Control*, vol.50, no.5, pp.655-661, 2005.